Modelling snowpack stability from simulated snow stratigraphy: Summary and implementation examples

Léo Viallon-Galinier, Pascal Hagenmuller, Benjamin Reuter, Nicolas Eckert

Available online at www.sciencedirect.com
ScienceDirect
CRST
Cold Regions Science and Technology 00 (2022) 1–32

Modelling snowpack stability from simulated snow stratigraphy: summary and implementation examples

Léo Viallon-Galinier[a,b,c], Pascal Hagenmuller[a], Benjamin Reuter[a,d], Nicolas Eckert[b]

[a] *Univ. Grenoble Alpes, Université de Toulouse, Météo-France, CNRS, CNRM, Centre d'Études de la Neige, Grenoble, France*
[b] *UR ETNA, INRAE, Université de Grenoble Alpes, France*
[c] *École des Ponts, Champs-sur-Marne, France*
[d] *WSL Institute for Snow and Avalanche Research SLF, Flüelastrasse 11, 7260 Davos Dorf, Switzerland*

Abstract

Information on snowpack stability, i.e., on the propensity for failure initiation and crack propagation in a weak layer, is essential for forecasting snow avalanches. To complement field observations, snow cover modelling provides information otherwise unavailable on the present and future state of the snow cover, and can be used to evaluate snowpack stability. The main goal of this paper is to summarize the broad spectrum of models to assess snowpack stability from simulated snow profiles. The basic mechanical concepts behind these stability models include: the maximum stress criterion which characterizes the failure initiation propensity and the critical crack length to evaluate the crack propagation propensity. However, many subtle differences between models, mainly due to additional expert rules or the effective implementation of the concepts, can be confusing. We try to disentangle this diversity in this summary. We discuss the differences and also present an overview of the mechanical parameterizations of snow material properties such as strength or stiffness as they are a key ingredient for stability modelling. In addition, we apply the stability models to typical and simplified snow profiles in order to illustrate the influence of the underlying assumptions and the model sensitivity to the mechanical input. As we point out scientific challenges and model limitations, the examples we discussed can provide guidance on the interpretation of similar model results. Moreover, we draw some guiding lines for future research concerning snowpack stability assessment based on snow cover modelling.

Keywords: snow, snowpack stability, stability indices, snow mechanical properties

1. Introduction

Avalanches are a significant issue in mountain areas by threatening outdoor recreationists and infrastructure (Wilhelm et al., 2000; Stethem et al., 2003). Assessing avalanche hazard is therefore important in these areas and, to this end, several countries rely on operational forecasting services (LaChapelle, 1977; Morin et al., 2019).

Avalanche hazard forecasting requires information about the current state of the snowpack, which is the result of the meteorological history, and its future evolution under meteorological conditions (LaChapelle, 1977). To fulfill these requirements, two main sources of information have been generally used. On one hand, observation networks have been developed with the goal of regularly reporting meteorological conditions and vertical profiles of snow properties including estimations of grain shape and size, density, humidity or temperature (Pahaut and Giraud, 1995; Fierz et al., 2009). On the other hand, numerical snow cover models (Morin et al., 2019), such as Crocus (Brun et al., 1989; Vionnet et al., 2012), Snowpack (Bartelt and Lehning, 2002; Lehning et al., 2002b,a) or Sntherm (Jordan, 1991), can describe the evolution of physical properties of the snowpack with time. Both approaches aim at providing detailed snowpack stratigraphy, including vertical profiles of physical and mechanical properties, which is the basis for snowpack stability analysis, but they differ in spatial and temporal resolution.

Slab avalanches, whether they release naturally or are artificially triggered, result from a sequence of processes occurring in the snowpack (e.g. Schweizer, 2017). First a failure initiates in a weak layer, this can happen progressively and lead to natural release or rapidly when caused by an external trigger (e.g. a skier). The initial failure can grow into a crack which will start self-propagating if the crack reaches a critical size. If not arrested by the tensile failure of the slab, the crack then propagates dynamically (Bergfeld et al., 2021b). Finally, an avalanche releases if the basal friction within the damaged weak layer is insufficient to prevent sliding of the slab on its substratum. The first processes, namely failure initiation and onset of crack propagation, describe the snowpack stability at the point scale, which is paired with spatial information for avalanche forecasting (Statham et al., 2018). We here focus on snowpack stability at the point scale. Low snowpack stability means the snow layering is prone for failure initiation and crack propagation.

Point stability can be observed in the field with stability tests, such as the compression test (van Herwijnen and Jamieson, 2007), the extended column test (Simenhois and Birkeland, 2009), the rutschblock (Föhn, 1987a) or the propagation saw test (Gauthier and Jamieson, 2008). Besides, observed snowpack profiles can be interpreted in terms of stability by applying expert rules (Jamieson and Schweizer, 2005; Coléou and Morin, 2018). A complementary approach is to use models computing instability indicators that describe the processes leading to avalanche release, which would facilitate interpretation of snow cover model output for avalanche hazard assessment and numerical avalanche forecasting (Morin et al., 2019).

Since the pioneering work of Roch (1966a), several mechanical models were developed to assess snowpack stability from either simulated or measured vertical profiles of snow properties. Schweizer (1999) or Schweizer et al. (2003) reviewed the processes involved in avalanche formation. Podolskiy et al. (2013) compiled the different methods used to model a simplified slab structure with the finite element method. However, to the best of our knowledge, there is no recent review of the models used to assess snowpack stability from snow profiles even if this field has evolved quickly in the past decade.

The aim of this paper is to provide an overview of existing methods to compute stability indicators from detailed snow stratigraphy based on a mechanical analysis. More precisely, we focus here on mechanical models which provide point stability information from modeled snow cover data. Technically speaking, it means that snow layer properties from the snow cover model are used as input of a mechanical model which provides indicators of stability. We only consider snow cover models which aim at representing the whole layering of a snowpack, such as SNOWPACK or Crocus, and mechanical models with demonstrated applicability to this kind of snow cover models.

We provide a snapshot of currently applied mechanical models in Section 2. These models generally rely on the information on the mechanical properties of the snow layers. Commonly used parameterizations of the mechanical properties are thus detailed in Section 3. Then the main stability models are applied to different typical situations to point out their strengths and limitations in the light of the underlying assumptions (Section 4). Finally, we conclude and discuss some guiding lines for future research.

2. Stability models

Stability tests mimic the processes involved in avalanche release and have long been used as snow stability information at the point scale (e.g. Föhn, 1987b). Extending from those concepts, mechanical models have been developed and have improved our understanding of the processes contributing to snow instability (Figure 1a). In particular, fracture mechanics helped formalizing the distinction between failure initiation and crack propagation. In this section, we review different models that have been used to characterize snow stability at the point scale.

Snow stability models can be separated into two groups: purely mechanical models and expert models. The first group consists of models that rely on material properties and a mechanical theory. For instance, some failure initiation models derive from the maximum stress criterion, which assumes that a material fails when the stress in a material element exceeds its strength. The second group comprises the so-called expert models. These models have a mechanical basis, but also include empirical thresholds and adjustments which do not derive from a mechanical theory but expert knowledge. For example, the maximum stress criterion can be adjusted by considering differences between the properties of adjacent layers (e.g. Schweizer et al., 2006).

Stability models of each group are listed in Tables 1 and 2 according to the main mechanical criterion they rely on. In particular, we present the input variables specifically required to run the model (in addition to basic layer properties such as thickness, density and slope angle). The main goal is to refer to the original study which describes the model and its theoretical basis. Besides, we direct the reader to applications of the model to snow cover simulations. Model evaluations are also cited when available and the model computation complexity is roughly estimated. We try to briefly summarize the important computation steps in equations where possible. The notations used are summed up in Section 6.

2.1. Purely mechanical models

The purely mechanical models are listed in Table 1 with references to theoretical work on each model. They are presented according to the main processes they represent: failure initiation or crack propagation. We focus in this section on the concepts of presented models. Practical implementations details are discussed further in Section 3.

2.1.1. Failure initiation models

The natural strength-stress ratio S_n, often called natural stability index, is a mechanical criterion comparing the shear strength τ_c of the weak layer to the shear stress τ due to the weight of the overlying snowpack: $S_n = \tau_c/\tau$. This concept was introduced by Roch (1966a) and further evaluated by Föhn (1987a).

A model also taking into account the skier-induced stress $\Delta\tau$ in addition to the snow load was developed by Föhn (1987a): $S_a = \tau_c/(\tau + \Delta\tau)$. This ratio is referred to as the skier stability index. For consistency, we call it the skier strength-stress ratio. The additional stress due to a skier is generally calculated based on the analytical solution for load distribution in an elastic half space (Boussinesq, 1885), with some simplifications and empirical adjustments based on grain shape or bond characteristics (e.g. Lehning et al., 2004; Giraud et al., 2002). Finite element models can also capture the full distribution of the skier induced stress in a layered snowpack (e.g. Habermann et al., 2008; Gaume and Reuter, 2017). In both cases, the calculation of $\Delta\tau$ assumes that snow is an elastic material and, for instance, plastic skier penetration on top of the snowpack cannot be accounted for.

In artificial triggering, an external load is required to fail the weak layer which may subsequently lead to an avalanche. Combining external load and the associated material property (strength) through dimensional analysis, Reuter et al. (2015) introduced a failure initiation criterion directly relating the skier-induced stress $\Delta\tau$ to the shear strength of the weak layer τ_c : $S_r = \tau_c/\Delta\tau$, omitting the stress due to the load of the slab. Here, we call it the external strength-stress ratio.

The damage process preceding natural avalanche release can be slow with the progressive failure of individual bonds in the weak layer. If the rate of bond cracking overcomes the rate of bond healing through sintering, a failure

can initiate in the weak layer (Capelli et al., 2018). To quantify this damage process potentially leading to failure, Lehning et al. (2004) introduced the so-called deformation rate stability index S_d, here called the deformation rate ratio. This index is based on the theoretical work of Nadreau and Michel (1986) and compares the stress at the bond scale σ_b to the bond strength σ_{b_c} (both computed in the model SNOWPACK): $S_d = \sigma_b/\sigma_{b_c}$.

Natural, skier, external and deformation rate ratios (S_n, S_a, S_r and S_d, respectively) describe failure initiation. The ratio S_d also includes the stage prior to formation of initial crack: the progressive damage of bonds into a macroscopic crack. All are oriented as stability indices, that is to say low values are associated to poor stability whereas high values are associated to stable conditions.

2.1.2. Crack propagation models

Failure initiation is required to release an avalanche but it is not sufficient (van Herwijnen and Jamieson, 2007). Only if the initial crack reaches a critical size, it may become self-propagating. Models describing the conditions at onset of crack propagation employ the concept of the critical crack length (e.g. Anderson, 2017).

Although propagating cracks were observed in the field and concepts suggested (e.g. McClung, 1979), it was only after specific field tests were introduced such as propagation saw test (PST) (Gauthier and Jamieson, 2006) and analyzed (Sigrist and Schweizer, 2007) that crack propagation models were developed for the onset of crack propagation. The onset of crack propagation corresponds to the state where the specific fracture energy of the weak layer equals the energy release rate of the material around. In other words, it refers to the equilibrium between the fracture energy required to extend the crack in the weak layer and the strain energy released in the material surrounding the weak layer that deforms during this process. The models presented here assume that energy release is due to elastic bending and change in potential energy of the slab. The first estimations of critical crack length assumed a homogeneous slab to compute the strain energy release (Sigrist et al., 2006; Heierli et al., 2008; Schweizer et al., 2011). Accounting for slab layering (Reuter et al., 2015) and enhancing the formulation of strain energy with finite element simulations (van Herwijnen et al., 2016), these authors derived the critical crack length from measured penetration profiles and showed that it is related to the length directly measured in propagation saw tests (Reuter and Schweizer, 2018). When we calculate the critical crack length, denoted a_c, we use the equations described by Schweizer et al. (2011).

An alternative approach considering shear induced stresses at the crack tip and their influence on the weak layer has been developed by Gaume et al. (2017). Based on discrete element simulations, they related the critical crack length to the slab and weak layer properties with an analytical formula (see eq. 9 in Gaume et al., 2017). Note that this formula depends on the thickness of the specific weak layer used in this study and could somehow be related to the collapse height of the weak layer. More recently, this equation was adjusted with correction factors to fit field

measurements to snowpack simulations and fill the gap between the layer thickness corresponding to the snow cover model vertical resolution and the one required by Gaume's parameterization (Richter et al., 2019).

Once a crack starts to propagate, a vertical tensile fracture through the slab may still arrest the crack in the weak layer. In order to quantify the capacity of the slab to support crack propagation in the weak layer, the slab tensile criterion T compares the tensile strength of the slab layers to the tensile stress due to slab bending at the onset of crack propagation, i.e. when the critical crack length is reached (Reuter and Schweizer, 2018). It represents the portion of the slab where the tensile stress exceeds the tensile strength, at the onset of crack propagation.

In the conceptual representation of avalanche formation (Figure 1b) the indices a_c, a_g and T refer to the process of crack propagation. Low values of the critical crack length a_c or a_g indicate high crack propagation propensity. Low values of the slab tensile criterion T indicate sufficient support of the slab for crack propagation. Indices describing the dynamic phase of crack propagation haven't been suggested, yet, as the associated theory and measurements are still under development (Bergfeld et al., 2021b).

The required input to calculate the described snow instability indices varies. Whereas the natural strength-stress ratio just requires weak layer strength, slope angle, slab thickness and average slab density, computation of the critical crack length or the slab tensile criterion can require more input variables and can be computationally more expensive. Moreover, the obtained indices also depend on the mechanical material properties computed at the layer scale. Hence, in section 3, we briefly discuss different parameterizations that are commonly used with the described snow stability indices.

2.2. Expert models

A list of mechanical models including expert knowledge is given in Table 2. The expert models are all somehow based on a shear strength-stress ratio representing failure initiation complemented with expert rules related to other contributing factors of avalanche formation such as propagation propensity and to the temporal evolution of the snow cover (Figure 1b).

The Structural Stability Index (SSI) is based on the skier ratio S_a, but also considers snow structural properties of the weak layer and its adjacent layers to refine the estimate of snow instability and to help identify weak layers. The skier ratio is adjusted by hardness and grain size differences between the weak layer and the adjacent layers (Schweizer et al., 2006). Typically, marked vertical differences of structural properties are related to lower stability.

The MEPRA index called "natural hazard" R_{nat} combines the natural strength-stress ratio S_n with empirical rules to an index describing the danger related to natural avalanche release on a 6-level scale. Expert rules concern the amount of new snow and snow wetness, which represent the two main drivers of natural avalanche activity. Moreover,

the hazard level is adjusted according to the temporal evolution of the snow cover to account for the short time persistence of natural instabilities (Giraud et al., 2002; Lafaysse et al., 2020).

The MEPRA index called "accidental hazard" R_{acc} blends the skier strength-stress ratio S_a with complex rules into an index describing the danger related to artificial triggering on a 4-level scale. These rules include the identification of a cohesive slab, sitting on a weak layer with typically composed of depth hoar, faceted crystals and precipitation particles and characterized by low values of S_a. The hazard associated with this weak layer is then estimated with additional expert rules (Giraud et al., 2002; Lafaysse et al., 2020).

Table 1: Summary of purely mechanical models, sorted by theoretical stability models. The first column presents the model and the original publications. The second column guides the reader to the references with the practical implementations and also lists the required input parameters (bullet points in italics) in addition to slope angle, the density and the thickness of the layers. The last column guides the reader to the evaluation of each model, when existing. Computational costs and implementation complexity is low except for the models including FEM simulations. The notations used are summarized in Section 6.

Model	Implementation and input parameters	Evaluation
Natural strength-stress ratio: $S_n = \tau_c/\tau$ Roch (1966a), Föhn (1987b)	**MEPRA** (Giraud and Navarre, 1995; Lafaysse et al., 2020) • *Shear strength* τ_c computed by snow cover model mainly from density and grain shape, with sophisticated adjustments based on sphericity, dendricity, grain size, liquid water content and history (Giraud and Navarre, 1995). **SNOWPACK** natural stability index or Sn38 (Lehning et al., 2004) • *Shear strength* τ_c computed by snow cover model from density and grain shape (Richter et al., 2019, Figure 2, therein). The *shear stress* τ is the shear component of the stress derived from the weight of the overlaying layers.	e.g. Nishimura et al. (2005)

Model	Implementation and input parameters	Evaluation
Skier strength-stress ratio: $S_a = \tau_c/(\tau + \Delta\tau)$ Roch (1966a), Föhn (1987b)	**MEPRA** (Giraud and Navarre, 1995; Lafaysse et al., 2020): • *Shear strength* τ_c computed by snow cover model mainly from density and grain shape, with additional adjustments for MEPRA (Giraud and Navarre, 1995) • *Skier induced stress* $\Delta\tau$ computed with an analytic function adapted to the grain shape of slab layers to represent the reduction of stress by hard layers (bridging effect) (Giraud and Navarre, 1995)	-
	SNOWPACK skier stability index or Sk38 (Lehning et al., 2004): • *Shear strength* τ_c computed by the SNOWPACK snow cover model with parameterizations of Jamieson and Johnston (2001) • *Skier induced stress* $\Delta\tau$: pre-defined function, taking into account ski penetration according to Jamieson and Johnston (1998) Some refinements to take into account normal stress and bond size dispersion have also been proposed by Lehning et al. (2004).	Schweizer et al. (2006); Nishimura et al. (2005)
External strength-stress ratio: $S_r = \tau_c/\Delta\tau$ Reuter et al. (2015)	**SNOWPACK** Failure initiation criterion (Reuter et al., 2022) • *Shear strength* τ_c from snow cover model (Richter et al., 2019) • *Skier induced stress* $\Delta\tau$: use of FEM for computing additional shear stress	Reuter and Schweizer (2018) Reuter and Bellaire (2018)

Model	Implementation and input parameters	Evaluation
Deformation rate ratio: $S_d = \sigma_b/\sigma_{b_c}$ Nadreau and Michel (1986)	**SNOWPACK** Deformation rate ratio (Lehning et al., 2004) : • *Critical stress in bonds* σ_{b_c} given by the model (Lehning et al., 2002b) • *Stress in bonds* σ_b derived from output of the snow cover model as: $\sigma_b = -p\tan(abs(\dot{\epsilon}_b))\sqrt{\frac{1-p}{p-\sigma_{0_{ice}}}}$ with pressure in bonds p computed as (Nadreau and Michel, 1986) with modelled temperature	-
Critical crack length a_c Sigrist et al. (2006) Heierli et al. (2008)	Critical crack length based on beam theory where a_c is the solution of a polynomial equation (Schweizer et al., 2011, see eq. 4). van Herwijnen et al. (2016) further developed this approach with FEM to account for size effects. Adapted by Reuter and Bellaire (2018) to be used after the SNOWPACK model. • *Weak layer fracture energy* w_f estimated from modelled shear strength (Reuter and Bellaire, 2018; Gaume et al., 2014). • *Slab equivalent modulus* E_{eq} determined by an FEM model (Reuter et al., 2015) where each layer is assumed to be elastic with a modulus computed with an exponential law on density (Scapozza, 2004)	Reuter and Bellaire (2018)

Model	Implementation and input parameters	Evaluation
Alternative critical crack length: $a_g = \sqrt{\frac{E'DD_{wl}}{G_{wl}}} \frac{-\tau + \sqrt{\tau^2 + 2\sigma(\tau_c - \tau)}}{\sigma}$ Gaume et al. (2017)	Applied by Schweizer et al. (2016b) and Richter et al. (2019). Simplified by (Richter et al., 2019) • *Slab equivalent modulus* E_{eq} determined by FEM modelling (Schweizer et al., 2016b) on elastic modulus determined with an exponential low on density (Scapozza, 2004) • *Shear modulus of the weak layer* G_{wl} set at a constant value, 0.5 MPa in Schweizer et al. (2016b)	Richter et al. (2019) Schweizer et al. (2016b)
Slab tensile criterion: T Reuter and Schweizer (2018)	**SNOWPACK** Tensile criterion (Reuter and Schweizer, 2018, see eq. 1), with implementation by Reuter and Bellaire (2018) • *Tensile strength* σ_c estimated with (Jamieson and Johnston, 1990) • *Tensile stress* based on FEM computation to determine tension at onset of crack propagation	Reuter and Bellaire (2018)

Table 2: Summary of expert stability models

Model	Implementation	Evaluation
MEPRA indices: R_{acc} R_{nat} Giraud et al. (2002)	**MEPRA** hazard indices (Vionnet et al., 2012), based on criteria S and S_a with : • *shear strength*, • *penetration resistance*, • *grain shape*, • *temperature* • *liquid water* all output of the snow cover model for each layer (Vionnet et al., 2012; Lafaysse et al., 2020)	-
SSI stability index Schweizer et al. (2006)	**SNOWPACK** based on Sk38 (Schweizer et al., 2006). Uses thresholds on variations between adjacent layers of: • *Hardness* • *Grain size* all output of the snow cover model for each layer (Bartelt and Lehning, 2002; Lehning et al., 2002b)	Schweizer et al. (2006)

3. Mechanical parameters

Detailed snow cover models such as Crocus or SNOWPACK simulate snow layer properties such as thickness, density, temperature, liquid water content and various grain shape proxies (e.g. Vionnet et al., 2012; Bartelt and Lehning, 2002). However, the stability models presented in the previous section also require mechanical properties as presented in the second column of Table 1. The link between snow cover model properties and mechanical properties such as weak layer strength, or slab equivalent modulus thus rely on additional parameterizations, which are not specific to the considered snow cover model. A variety of parameterizations exists for the same mechanical parameter,

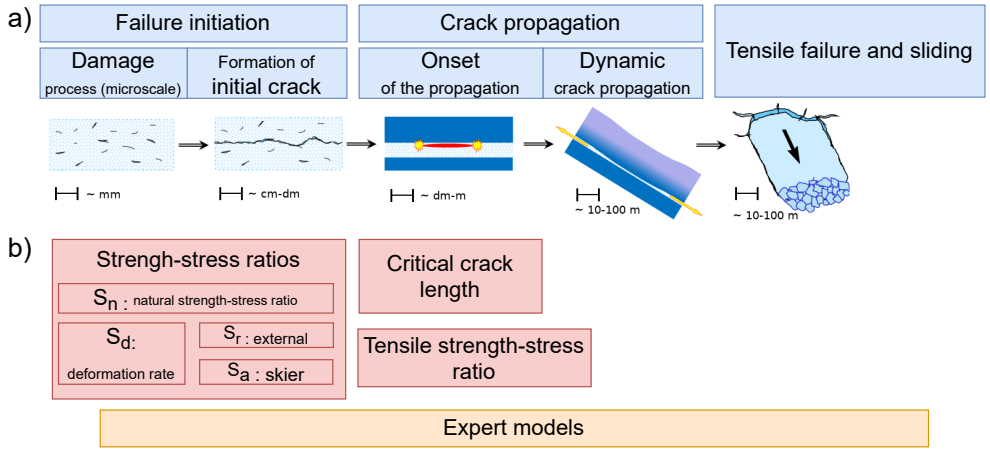

Figure 1. (a) Processes involved in avalanche formation according to Schweizer et al. (2016a) and (b) classification of stability models according to the processes they represent.

as for instance, for the skier-induced stress that represents the bridging effect in Crocus (Giraud et al., 2002) or the skier penetration in SNOWPACK (Lehning et al., 2004) (see Table 1). The choice of such parameterizations can have a significant impact on the results of the stability models. Without being exhaustive, we provide an overview of the diversity of the existing methods to obtain the properties required for computing stability indices (Figure 2).

The input to the stability models includes properties simulated by snow cover models (e.g. thickness, density and grain shape), mechanical properties for a particular layer (e.g. layer shear strength, see Figure 2a) and mechanical properties depending on many layers of the stratigraphy (e.g. slab equivalent modulus, Figure 2b).

3.1. Mechanical properties per layer

The mechanical properties required per layer are material properties which do not depend on the surrounding layers. They include elastic and failure properties. They are mainly determined in field or lab measurements that are then used to fit more general parameterizations.

The **elastic modulus** E describes the amount of reversible deformation for a given stress and has been measured with various techniques at different strain rates. Mellor (1974) reported values of modulus measured with different techniques and strain rates from 10^{-6} to 10^{-2} s^{-1}. Camponovo and Schweizer (2001) used a rheological setup to derive elastic shear modulus while Gerling et al. (2017) used wave propagation to measure elastic modulus at high strain rates. Based on these measurements, different parameterizations emerged, mainly as functions of density. They include linear or power relations of density, temperature or strain rate (e.g. Smith, 1965), power laws of density (e.g. van Herwijnen et al., 2016; Gerling et al., 2017) and exponential laws of density (e.g. Scapozza, 2004). Another way of estimating snow elastic properties is from microtomography images and numerical modelling of the material behaviour from ice and air properties (e.g. Köchle and Schneebeli, 2014; Wautier et al., 2015; Srivastava et al., 2016).

Elastic properties also include the **Poisson's ratio** ν which describes the deformation perpendicular to the loading direction. It is either usually chosen as a constant value in the typical range [0.25, 0.3] (Podolskiy et al., 2013) or determined from a density parameterization (Mellor, 1974; Sigrist et al., 2006).

Strength is a measure of the maximum stress that a material can support before starting to fail. For avalanche formation, considering different loading directions is important: shear or compressive strength of the weak layer for failure initiation and tensile strength of the slab during crack propagation (Roch, 1966a; Bobillier et al., 2021; Reuter and Schweizer, 2018). Different measurement techniques such as the rotating vane, the shear or tension frame, have been used in the field or in the lab (Mellor, 1974). Based on these measurements, power laws on density, sometimes specific to some grain shapes, have been determined (Perla et al., 1982; Jamieson and Johnston, 1990, 2001; Chalmers and Jamieson, 2001). For shear strength, adjustments accounting for normal load have been developed by (Jamieson and Johnston, 1998) and (Zeidler and Jamieson, 2006). A combination of such parameterizations are currently used in snow cover models (Lehning et al., 2004; Giraud et al., 2002).

Fracture energy corresponds to the energy per unit surface required to grow a crack. It is also related to the fracture toughness which describes the critical stress intensity at the crack tip (Griffith, 1921). The fracture energy was derived from experimental propagation tests with finite element modelling (Schweizer et al., 2011) or by measuring the deformation of the slab with particle tracking velocimetry (van Herwijnen et al., 2016). In addition, Reuter and Schweizer (2018) presented an empirical relation relating the snow micropenetrometer force to the fracture energy. In the lab, the fracture toughness was measured on notched beams composed of typical slab snow but not on weak layer snow (Schweizer et al., 2004; Kirchner et al., 2002).

3.2. Non local properties

The non-local properties are the **skier induced stress** $\Delta\tau$, the **slab equivalent modulus** E_{eq} and the **shear stress** τ. For their computation, mechanical properties of several layers are important. The skier-induced stress can be computed from an analytical solution (e.g Boussinesq, 1885) or estimated, for instance with a piecewise linear approximation (e.g. McClung and Schweizer, 1999) or with finite elements (e.g. Jones et al., 2006). The slab equivalent modulus is the result of a homogenization of the mechanical behaviour of the slab, assuming that in the specific loading situation, the slab deforms as a homogeneous material with elastic modulus E_{eq}. An estimate of the slab equivalent modulus can be obtained by an analytic averaging method (Sigrist, 2006; Monti et al., 2016) or by finite element modelling (e.g. Reuter et al., 2015). Full representation of snow stratigraphy by finite elements is expected to provide more accurate estimates but at the cost of longer computation times compared to bulk average for instance that do not account for order of layers (e.g. Habermann et al., 2008; Monti et al., 2016). A simple approach is to use the average of properties over layers (taking into account thicknesses) (Sigrist et al., 2006). The benefit of more

complex computations has to be weighted in particular in the light of the uncertainties carried out by the choice of parameterization of mechanical parameters per layer. The shear stress is derived from the weight of the overlying snowpack, always computed as the sum of the product of thickness and density of the layers above the weak layer and acceleration due to gravity.

3.3. Limitations of the parameterizations

The presented parameterizations mainly rely on experimental work and provide straightforward methods to compute mechanical properties from snow cover simulations. However, snow is a very fragile material (Kirchner et al., 2002) which limits sampling and testing, and presents different microstructural patterns due to very active metamorphism (Hagenmuller, 2014). Therefore, these parameterizations based on experimental work ineluctably have limitations.

Most of the presented parameterizations only rely on density as the main (or unique) descriptor of the snow microstructure (e.g. Keeler and Weeks, 1968; Scapozza, 2004; Schweizer et al., 2011) which cannot fully describe its complexity (Shapiro et al., 1997). Moreover, the parameterizations often do not take into account temperature, liquid water content or the loading conditions such as the strain rate and the loading direction, which are critical for the material behaviour in some cases (Mellor, 1974; Denoth, 1980; Shapiro et al., 1997).

Some properties are also difficult to measure or even some samples are difficult to carry to the lab, especially for weak snow (precipitation particles, depth hoar or surface hoar, for instance) (Reiweger and Schweizer, 2010; Walters and Adams, 2014). This limits the number of measurement points on such snow. The measurements used for fitting parameterizations do not cover all snow types. Numerical experiments based on tomographic images can help to characterize fragile snow types (e.g. Hagenmuller et al., 2014, 2015; Mede et al., 2018). Nevertheless, these tomography-based models are mainly limited to elastic properties and strength values and were simulated for a small number of samples.

Models estimating the crack propagation propensity require the slab equivalent modulus to represent slab deformation. The crack propagation models rely on the idea that, at the onset of crack propagation, the energy for crack extension in the weak layer equals the change of gravitational potential energy and the strain energy corresponding to the deformation of the overlaying slab (e.g. van Herwijnen et al., 2016). Hence, the commonly made assumption is that the mechanical behavior of the slab can be approximated by linear stress-strain relations with an equivalent modulus (Reuter et al., 2019). This equivalent modulus must not be related to the elastic modulus of snow as their definitions from a material science point of view differ. Stability indicators may require equivalent modulus representing the whole deformation rather than the well-defined material property. This assumption on the snow deformation regime

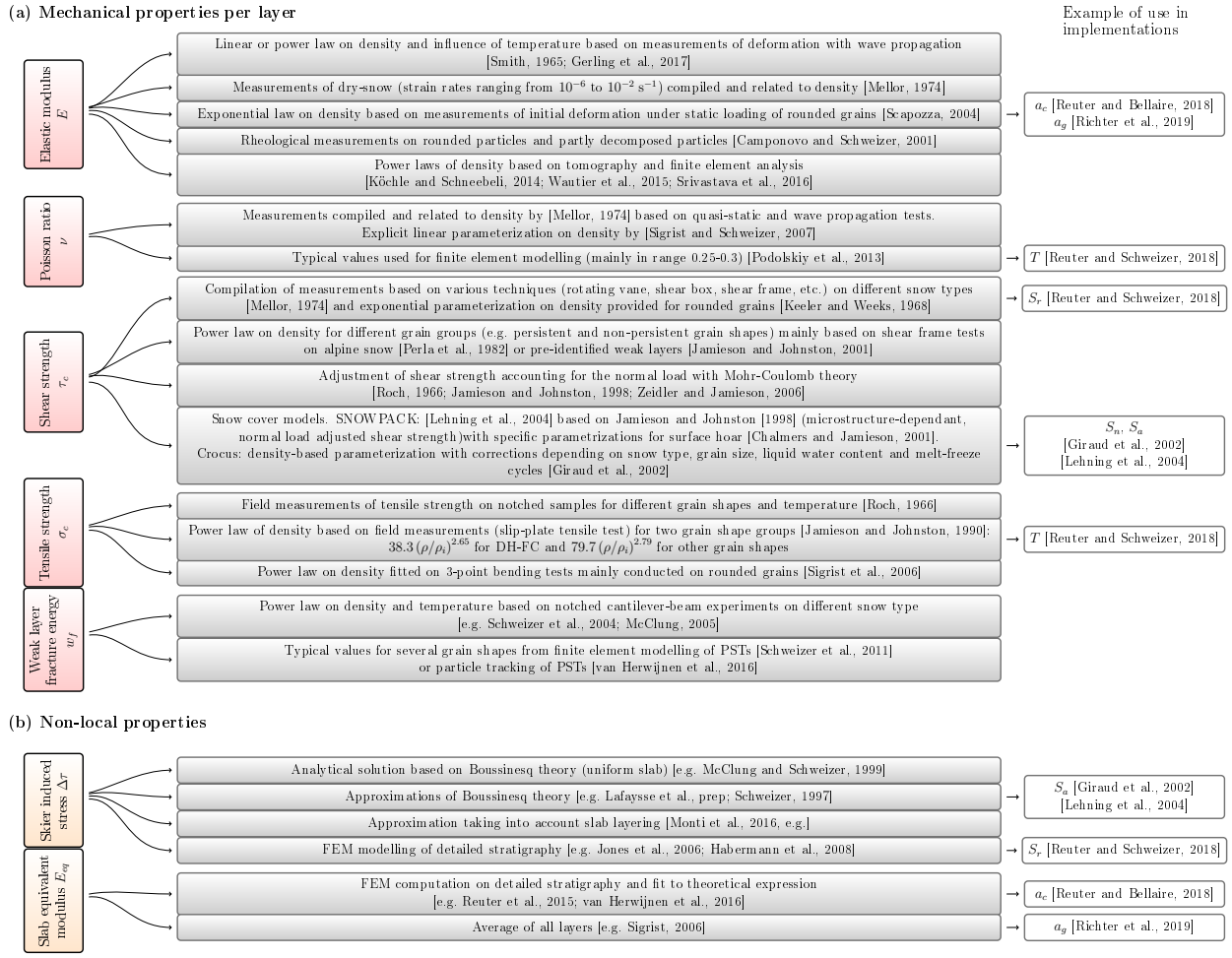

Figure 2. Map of the (a) mechanical properties per layer (red) or (b) non-local properties (orange). An overview of associated methods to determine mechanical properties from snow cover model output is given in the second column (grey).The stability models presented in Table 1 can be used with any of these mechanical parameterizations. However, the implementations cited in Table 1 used specific parameterizations, which are indicated in the last column of this figure.

can also lead to inconsistency in weak layer fracture energies depending on the chosen measurement techniques as discussed in LeBaron and Miller (2016).

4. Illustration

We applied the models from Section 2 to simplified snow profiles. Comparing their results allows for a short sensitivity analysis to assess how the models may describe the process of avalanche release and to emphasize their underlying assumptions. The goal is neither to provide an exhaustive sensitivity analysis of the different models nor to evaluate the models but we guide the reader to dedicated literature.

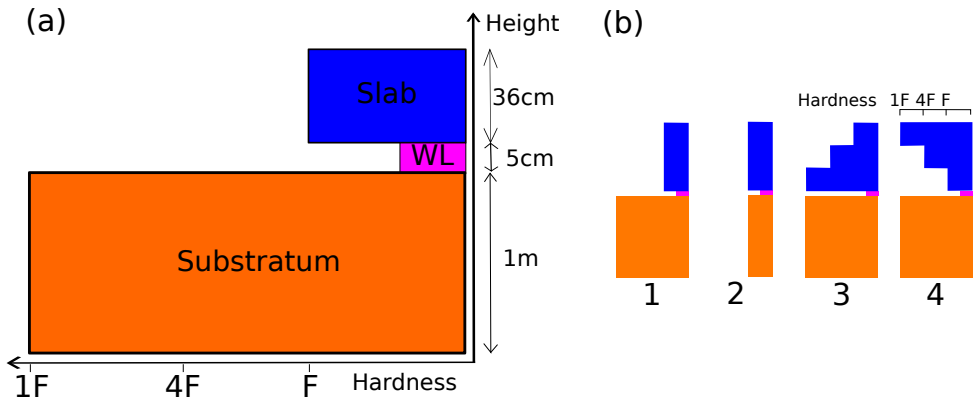

Figure 3. (a) Simplified snowpack stratigraphy, including three parts (substratum, weak layer (WL), slab) and (b) four simplified snow profiles from Habermann et al. (2008).

4.1. Methodology

4.1.1. Selected models

For illustration, we selected a subset of the stability models presented in Section 2. We chose models which require simple physical quantities (layer thicknesses, density or hardness...) and do not show expert models. In particular, S_d is based on the grain bond size which is a variable specific to SNOWPACK and was therefore not considered. Overall, we considered three strength-stress ratios namely S_n, S_r, S_a, two critical crack lengths a_c and a_g and the slab tensile criterion T. The onset of crack propagation used for the ratio T is here defined with the critical crack length a_c.

4.1.2. Selected snow profiles

We applied the stability models to a set of snow profiles inspired by Habermann et al. (2008) for a slope angle of 38°. Figure 3 presents the basic geometry of these profiles, composed of a slab, a weak layer and a substratum. Each layer is described by its density, hardness and elastic modulus according to Habermann et al. (2008) (see Table 3).

We also considered the temporal evolution of a snow profile after a snowfall. The substratum has the same properties as in Figure 3a. On top, a snow layer with a thickness of 5 cm with an initial density of 50 kg m^{-3} acts as a weak layer. Snow falls at a 10 cm h^{-1} rate for 10 hours creating layers with an initial density of 100 kg m^{-3}. The snow settles under its own weight. Settlement is described with a viscous law $\frac{\mathrm{d}D}{D} = \frac{-\sigma}{\eta}\mathrm{d}t$ where σ is the normal load on each layer, D the layer thickness and η the viscosity. The viscosity η depends on density: $\eta = \eta_0 \frac{\rho}{c_\eta} e^{b_\eta \rho}$ with $\eta_0 = 7.6$ kg s^{-1} m^{-1}, c$_\eta$ = 250 kg m^{-3} and b$_\eta$ = 0.023 m^3 kg^{-1} as in (Vionnet et al., 2012).

4.1.3. Mechanical properties

To apply stability models other properties are required apart from thicknesses, density and elastic modulus. As shown in Section 3, numerous mechanical parameterizations exist. We selected the following ones, based on their

Table 3. Table of mechanical properties derived from hardness for each layer.

Layer hardness	Density (kg m^{-3})	Elastic modulus (MPa)
Weak layer (WL)	100	0.15
Soft (F)	120	0.3
Medium (4F)	180	1.5
Hard (1F)	270	7.5

simplicity and use in previous implementations:

- The shear strength of the weak layer was set to 500 Pa as this value is in the range measured by Jamieson and Johnston (2001).
- The tensile strength of the slab is derived from Jamieson and Johnston (1990).
- The weak layer fracture energy was set to 0.2 J m^{-2}, consistent with the range observed by Schweizer et al. (2011).
- The skier induced stress $\Delta\tau$ was computed according to McClung and Schweizer (1999).
- The equivalent modulus of the slab was estimated by the mean elastic modulus of the slab layers (e.g. Sigrist, 2006).

To illustrate the role of the slab layering (Section 4.3), we also computed the skier induced stress $\Delta\tau$ and the slab equivalent modulus E_{eq} with finite element simulations (Reuter and Schweizer, 2018). The slab equivalent modulus is computed by considering the deformation energy of the slab only and does not include the substrate. The strength-stress ratios S_{r_F} and S_{a_F} were simulated with finite element simulations. The critical crack length using finite element simulations for equivalent modulus is denoted a_{c_F}.

For temporal evolution, all mechanical parameterizations were set as in the previous paragraph except the elastic modulus, shear strength and weak layer fracture energy. The elastic modulus was computed as $E = 1.8 \cdot 10^5 \cdot \exp(\rho/\rho_0)$ (Pa) (Scapozza, 2004) with $\rho_0 = 67$ kg m^{-3} and shear strength as $\sigma_c = 14.5 \cdot \frac{\rho}{\rho_{ice}}^{1.73}$ (kPa) (Jamieson and Johnston, 1990). Given the lack of parametrizations of the weak layer fracture energy, we derived plausible values to describe the temporal evolution. We estimated the weak layer fracture energy as $\alpha \cdot \tau_c^2/E$ as this assumption has provided reasonable results in specific applications (see Birkeland et al. (2019, Equation 4) or Gaume et al. (2014, Equation B7)). The scaling coefficient $\alpha = 0.2$ J m^{-2} was chosen so that w_f is in the range observed by Schweizer et al. (2011). Hence, it can be regarded an order-of-magnitude best guess.

4.2. Homogeneous slab

We conducted a sensitivity analysis on the simplified stratigraphy presented in Figure 3a to discuss the influence of mechanical parameters in each stability model. This stratigraphy is used as a reference and six parameters (slab thickness, slab equivalent modulus, weak layer shear strength, weak layer fracture energy, weak layer thickness and weak layer elastic modulus) were altered one after the other. By doing so, we did not account for possible correlation between the different parameters. For instance, we do not consider that, in the field, a thick slab is on average denser and stiffer than a thinner slab. However, this is on purpose to discuss the processes that are represented or not by the different models and the influence of mechanical parameters on their results. The sensitivity analysis is first presented for the shear strength-stress ratios mainly representing the failure initiation processes, then for the critical crack length representing the crack propagation propensity and eventually for the slab tensile criterion (representing potential slab fracture breaking off crack propagation).

Shear strength-stress ratios are, as expected, affected by slab thickness and weak layer shear strength (Figure 4), in addition to the density of the slab (not shown). The shear strength-stress ratios S_n (natural), S_a (skier) and S_r (external) are sensitive to the slab thickness. A thicker slab means a heavier slab and consequently, a higher stress is induced in the weak layer, so a lower value of S_n is obtained. In contrast, the skier induced stress in the weak layer is reduced by a thicker slab and consequently leads to a higher value for S_r. The skier ratio S_a combines the two effects and hence presents a non-monotonic evolution with a maximum for a thickness of 0.5 m. The shear strength-stress ratios are proportional to the weak layer shear strength: they increase linearly with this parameter. The other parameters, weak layer thickness and weak layer stiffness, do not affect the shear strength-stress ratios. The natural ratio S_n is by definition only sensitive to the load of the overlying slab (stress) and to the strength of the weak layer. In contrast, the skier induced stress can be affected by the layering of the elastic modulus as shown by Habermann et al. (2008). However, in this sensitivity analysis we used an analytical expression for skier induced stress which only depends on depth and slope angle (McClung and Schweizer, 1999) and thus cannot capture the effect of layering.

The critical crack lengths, a_c and a_g, decrease with increasing slab thickness as this parameter affects slab bending and the subsequent stress concentration at the crack tip. The other way around, the critical crack length increases with slab equivalent modulus as stiff slabs deform less. Low values of weak layer strength ease failure initiation and facilitates crack propagation: a higher strength yields a larger critical crack length. Indeed, weak layer strength explicitly appears in the expression of a_g. However, a_c is not affected by weak layer shear strength as the mechanical parameter used in this stability model is the weak layer fracture energy. Indeed, a_c increases with weak layer fracture energy.

The weak layer thickness is also taken into account to compute a_g. When using a snow cover model, this thickness

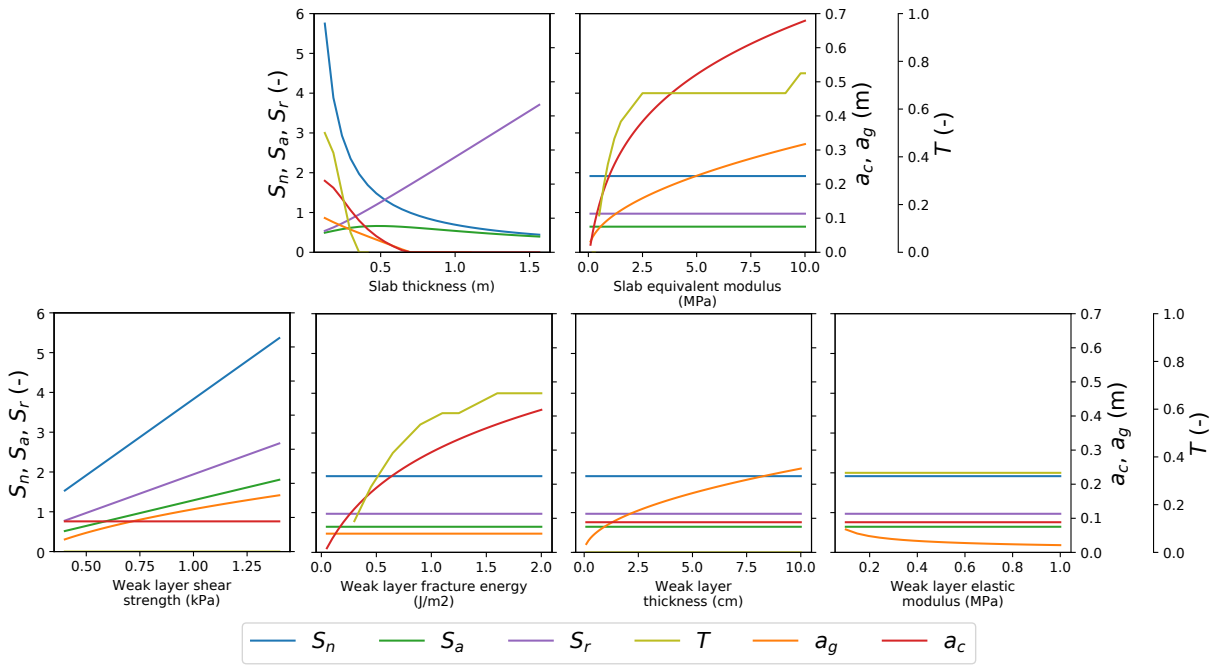

Figure 4. Sensitivity analysis of the stability models to their mechanical parameters on the simplified snow profile described on Figure 3a. Legend names refer to models described in Table 1.

does not refer to the simulated layer thickness (vertical resolution of the model) but rather to a "useful thickness" (Richter et al., 2019), probably related to the zone where the strain accumulates (Walters and Adams, 2014). Moreover, the critical crack lengths decrease with the weak layer elastic modulus, as the modulus affects the stress concentration at the crack tip. It is an explicit parameter in the expression of a_g and this effect is also indirectly captured by a_c with the chosen parameterization of the weak layer fracture energy w_f.

The slab tensile criterion T describes the ratio between tensile stress and strength in the slab at the onset of crack propagation, when critical crack length is strictly positive. It is highly related to the value a_c: the shorter the critical crack length, the smaller the unsupported part of the slab and the smaller the deformation. That means we obtain low values of tensile stress and low values of T.

4.3. Layered slab

We applied the different stability models to snow profiles with different slab layering (Figure 5). We first present the results for failure initiation, then for crack propagation.

The natural ratio S_n is only sensitive to the load of the slab. Values are the same for the profiles 1 and 2 and for the profiles 3 and 4 but the load is larger for the profiles 3 and 4 compared to the profiles 1 and 2. The external ratio S_r is only dependent on slab thickness since the skier stress distribution is computed with a very simple analytical

expression which neglects the potential impact of layering (McClung and Schweizer, 1999). The value of S_r is thus the same for all presented profiles. In contrast, the external ratio S_{rF} relies on finite element simulations and is able to account for the impact of snow layering, including the substratum (e.g. Habermann et al., 2008; Thumlert and Jamieson, 2014). The value of S_r is slightly lower for a stiffer substratum (profile 1 compared to profile 2) and significantly lower for density increasing with depth in the slab (profile 3) in contrast to a slab density decreasing with depth (profile 4). In the latter case, note that the model for S_r does not account for any potential skier penetration in the snowpack. Therefore, the effect of a hard layer at the surface might still be under-estimated by this model (Habermann et al., 2008). The skier ratios S_a and S_{aF} exhibit little variations, with the slab layering or with the elastic modulus of the substratum, with values ranging between 0.5 and 0.6 for the provided examples.

The critical crack length a_g is related to both slab equivalent modulus and load. Layering is not accounted for since the slab modulus is here simply computed as the average of all layers. The values of a_g appear to be almost the same in all profiles. Indeed, the effects of additional load are here counterbalanced by the effects of an increased stiffness. In contrast, a_c exhibits more variations with the different snow profiles. As expected, the values of the critical crack length do not depend on the substratum (profiles 1 and 2) as it is not represented in the models. Moreover, slab properties are averaged in the computation of a_c and a_g, and thus the models do not represent the layering of the snowpack (profiles 3 and 4). Yet, a finite element simulation accounts for the layering of the slab in the computation of a_{cF}. Noticeably, in profile 4, where density decreases with depth, the critical crack length a_c is larger by a factor of 2.8 compared to a_{cF}, which is in agreement with the findings of Gaume and Reuter (2017). In profile 3, the critical crack lengths a_c and a_{cF} are very close, which shows that in this case averaging the elastic modulus to define the slab equivalent modulus may be sufficient. The values of a_c and a_g, i.e. the two different models of the crack length, are very different for profiles 3 and 4 (a_c = 26 cm, a_g = 5 cm). Sensitivity studies on a representative set of profiles help to assess how important it is to explicitly account for this layering, as done by e.g. Habermann et al. (2008) or Monti et al. (2016) for skier induced stress and Reuter and Schweizer (2018) for critical crack length. The slab tensile criterion T computed with FEM shows larger variations between the profiles. Being representative of the tensile stress in the slab, which often concentrates near the surface, T has a higher value for profile 3 with lower strength at surface than profile 4, but it is also higher than for a uniform slab (profiles 1 and 2, value of zero) as a higher elastic modulus for one layer will concentrate the stress. The value is also correlated to a_c: higher values are linked to higher values of a_c.

4.4. Temporal evolution

Finally, we applied the selected stability models to a typical new snow situation. The slab is initially composed of new snow falling on a non-persistent weak layer composed of very low density snow. The time-evolution of the

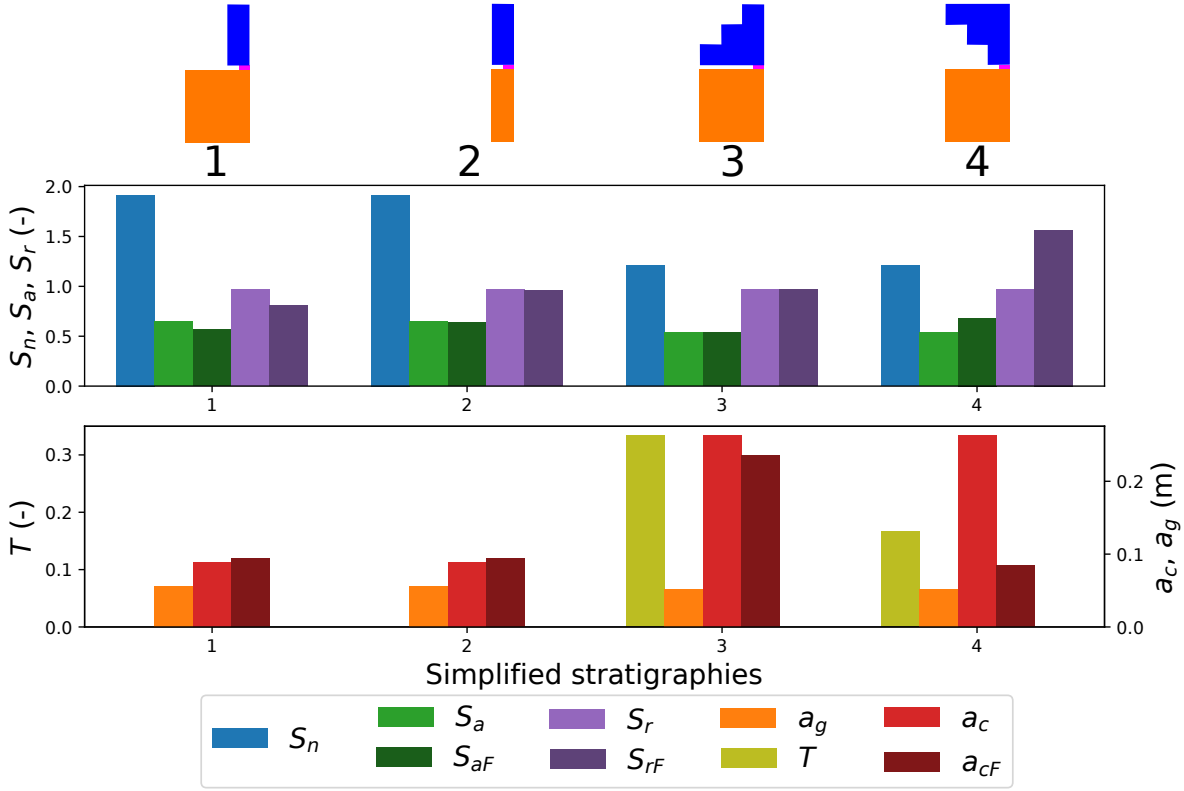

Figure 5. Sensitivity analysis of the stability models to different profiles presenting a heterogeneous layering. Legend names refer to models described in Table 1.

snowpack is studied up to five days after the snowfall (Figure 6).

The stress on the weak layer due to the new snow increases during the snowfall. When the snowfall ends, the stress remains constant, but other snowpack properties continue to evolve with time as snow settles: thickness decreases while density and strength increase, as measured by Roch (1966b). Consequently, the natural ratio S_n decreases during snowfall and then increases with weak layer hardening. By contrast, S_r and S_a increase during snowfall due to the increasing distance between the additional load (applied at surface) and the weak layer. This distance is then slightly reduced due to the settlement leading to a reduction of the increase rate of the values of S_a and S_r. In a real situation, the skier may penetrate the snowpack and the effective skier load may be higher at beginning due to skier penetration, which is not represented here (Schweizer and Reuter, 2015; Monti et al., 2016; Thumlert and Jamieson, 2014).

Both models of the critical crack length show decreasing values during snowfall due to the increased stress on the weak layer. After the snowfall, the values of the critical crack length increase, representing a stabilization which is mainly a consequence of snow settling leading to the stiffening of the slab and the strengthening of the weak layer. The stabilization following snow storms, with modelled settling, is faster immediately after the snowfall than later when processes slow down, which is consistent with observations of Birkeland et al. (2019). The values of T remain very close to zero, which indicates that the tensile stresses due to a crack of length a_c in the slab never exceed the tensile strength of the different layers. In other words, it means that tensile failure in the slab would be unlikely and crack would rather tend to keep propagating than be arrested.

5. Concluding remarks

We compiled different mechanical models which were developed to assess snowpack stability from simulated snow profiles. Two main mechanical concepts are behind the stability models: maximum stress criterion characterizes the failure initiation propensity and Griffith's energy criterion based on weak layer fracture energy allows to evaluate crack propagation propensity. However, model implementations present many subtle differences and the results are not all directly comparable, as models often complement each other (Figure 1). Moreover, some empirical rules are often included or different implementations of the mechanical properties co-exist. The main goal of this review was to explain the differences in a synthesis including the references to the relevant literature (Tables 1 and 2) and illustrative examples. We highlight the sensitivity of the stability models to the mechanical input such as strength or stiffness and thus also present an overview of the available mechanical parameterizations (Figure 2).

We provided an overview of the current state of research on snowpack stability assessment based on snow cover modelling, but also point out some scientific challenges and draw some guiding lines for future research.

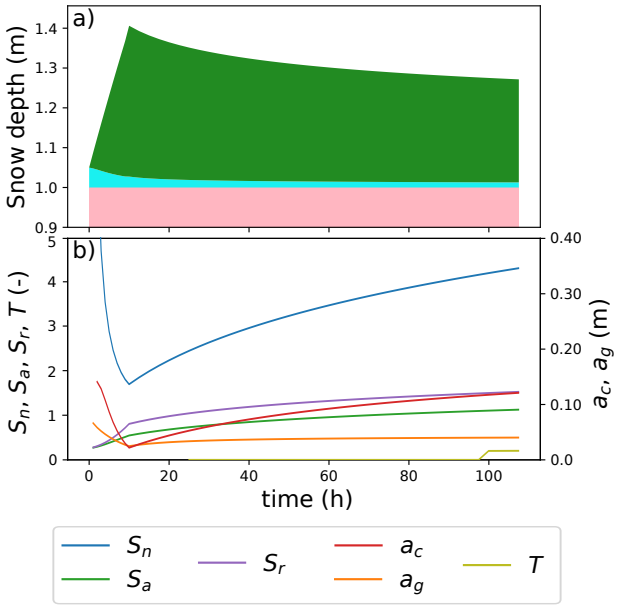

Figure 6. Temporal evolution of the snow depth (a) and of the associated stability models (b) during and after a snowfall. The slab (dark green) is composed of new snow with a moderate density (initial value of 100 kg m^{-3}). The weak layer (blue) is composed of very light snow (initial density of 50 kg m^{-3}). The slab and the weak layer evolve with time due to snow settlement. The substratum (pink) is composed of hard snow and do not evolve with time. Legend names refer to models described in Table 1.

It appears that all stability models share the same assumption that snow behaves as an elastic brittle material which can be represented with continuum and fracture mechanics. However, it has long been known that snow also exhibits visco-plastic behaviour (e.g. Narita, 1980). In practice, the assumption of brittle elasticity makes sense for many of the processes involved in avalanche formation but may still limit the scope of the presented models both for failure initiation and crack propagation. In particular, an elastic model cannot correctly represent skier penetration and thus may fail to correctly reproduce skier-induced stress. Empirical adjustments based on snow depth and density have been developed (e.g. Schweizer and Reuter, 2015; Reuter et al., 2015) but the associated theoretical framework remains to be evaluated. Besides, all crack propagation models presented above assume that the slab deforms in an elastic manner whereas energy may dissipate notably near the crack tip or in the slab itself. Even if the slab modulus may be adjusted to an effective value to reproduce the observed behavior, the chosen elastic framework can lead to discrepancies between the input parameters of the stability models and the measured values of material properties. For instance, the weak layer fracture energy ranges between 0.2 and 2.2 J m^{-2} when derived from propagation saw tests (van Herwijnen and Heierli, 2010; Schweizer et al., 2011; Bergfeld et al., 2021b) but is estimated around 0.05 J m^{-2} if derived from ice properties and 3D microstructure (LeBaron and Miller, 2016). This discrepancy is not a problem in itself but limits stability models to benefit from broader studies focusing on snow as a material.

To represent the different processes of avalanche formation that contribute to point stability, several indices have to

be combined (Figure 1). At least indices for failure initiation and crack propagation have to be considered simultaneously. Several studies proposed possible combination of stability indices, such as Reuter et al. (2015) who combined S_r and a_c or Reuter and Schweizer (2018) who added T. Gaume and Reuter (2017); Rosendahl and Weißgraeber (2019b) merged a failure stress condition and an energy condition for crack propagation. Besides, the presented stability models focus on failure initiation and on the onset of crack propagation, which corresponds only to the central part of the series of mechanical processes leading to avalanche release (Figure 1). So far, less attention was paid to the progressive damaging of the weak layer which can lead to the creation of an initial crack. After Conway and Wilbour (1999) had presented a time derivative based on natural strength-stress ratio, their model has long not been used with snow cover models, but very recently implemented to assess natural release from snow cover modelling (Reuter et al., 2022). Recent studies have investigated the competition between bond breaking and the healing due to sintering (Capelli et al., 2018) and their translation into material visco-plasticity (e.g. Puzrin et al., 2019). Explicitly adding time dependent processes in the stability models can eventually help to pinpoint natural avalanche activity and improve existing models (Brown and Jamieson, 2008). At the very end of the series of processes, dynamic crack propagation has seen more research more recently (e.g. Gaume et al., 2018; Bergfeld et al., 2021b). Trottet et al. (2021) suggested that once the crack has reached a "super-critical" size (larger than the size at the onset of crack propagation), the involved failure mechanism or mode might switch and affect the size of the avalanche release area. However this idea was challenged by the results of Bergfeld et al. (2021a). Research on the processes involved in the dynamic phase of crack propagation that follows the onset is ongoing. At last, even for point stability assessment, a minimal spatial homogeneity is assumed (at least on several meters), especially for crack length modelling whereas terrain or wind effects induce spatial heterogeneity of the snowpack (Gaume, 2012) and highly influence propagation results (Gaume et al., 2013). Detailed snow cover models are mainly 1D models and do not represent meter-scale spatial variability.

The most recent studies designed to understand the physics of avalanche formation mainly work with a simple two-layer stratigraphy composed of a homogeneous slab and a weak layer (e.g. Gaume et al., 2015; Bobillier et al., 2021; Rosendahl and Weißgraeber, 2019a). These models can thus not directly be applied to heterogeneous vertical snow profiles (see influence of layering in Figure 4). These models have either to be adapted to more complex snow profiles or an additional step is required to reduce the complex stratigraphy, for instance with the use of equivalent mechanical properties (Monti et al., 2016). Moreover, the substratum has been shown to influence snowpack stability. The mechanical properties of the substratum can modify the stress distribution especially in the weak layer just above (Habermann et al., 2008) and can also influence the crack propagation propensity since layering affects the stress distribution in the slab (e.g. Gaume and Reuter, 2017; Reuter and Schweizer, 2018). However, it appears from this

review that accounting for the substratum is not systematically taken into account in the stability models.

For understanding the concepts involved in avalanche formation, simplified stratigraphy (for instance with homogeneous slab) is of crucial help to separate between involved processes. However, for practical use in avalanche forecasting, the full stratigraphy is crucial as it can decide whether a weak layer fails for example. To get this stratigraphic information, both observed profiles or simulation (Schweizer et al., 2006) can be analyzed with expert rules to identify critical weak layers. Some stability indices have been developed specifically to identify weak layers prior to further stability analysis such as SSI (Schweizer et al., 2006). Other expert methods may also be used to identify weak layers such as the so-called lemons (Jamieson and Schweizer, 2005) or the tracking approach developed by Reuter et al. (2022).

The assessment of the snowpack stability highly depends on the knowledge of the material properties of the layers. There is a large variety of mechanical parameterizations (Section 3) and their choice affects the stability indices (Figure 4). This large variety is due to the complexity of snow as a material. In particular, mechanical properties are highly sensitive to temperature, liquid water content (e.g. Mellor, 1974) or the microstructure (e.g. Hagenmuller et al., 2015; Jamieson and Johnston, 1990). Moreover, the snow types which are critical to assess snowpack stability, for instance weak layers or snow near the melting point, are also difficult to measure. Thus, despite the amount of measurements available, there is no best practice for computing mechanical parameters for snow cover models (e.g. Podolskiy et al., 2013; Reuter and Schweizer, 2018). This limitation might also be linked to the rough representation of microstructure by snow cover models (or in observation reports) which may be insufficient to represent the evolution of mechanical properties.

If snow cover model output is used to run a stability model, also the meteorological forcing represents a source of uncertainty, which adds to the snow cover model uncertainty (e.g. Vernay et al., 2015; Lafaysse et al., 2017) and propagate to the finally computed stability indicators. Improving stability models needs to go with improvements of the snow cover models (e.g. Simson et al., 2021), including a better representation of snow microstructure or the explicit representation of the evolution of some mechanical properties (e.g. Hagenmuller et al., 2015). In any case, as they are computed from the output of snow cover models, stability indicators are sensitive to previous model parameterizations. A way to overcome these limitations is to use statistical tools to identify critical situations rather than only considering physically based models. These models range from simple statistical adjustments of the threshold on stability indicators (e.g. Reuter and Schweizer, 2018) to more advanced statistical methods such as random forests (e.g. Sielenou et al., 2021; Evin et al., 2021; Mayer et al., 2021). Besides, these techniques are versatile: they can be straightforwardly adapted to different versions of meteorological and snow models.

6. Notations used

Notations used are reported below:

- σ is the slope-normal stress in a snow layer
- τ is the slope-parallel (shear) stress in a snow layer
- τ_c is the shear strength of a snow layer
- σ_c is the tensile strength of a snow layer
- σ_b is the stress in bonds
- σ_{b_c} is the strength in bonds
- $\Delta\tau$ is the skier-induced stress
- D is the slab thickness
- D_{wl} is the weak layer thickness
- E denotes the elasitc modulus
- E_{eq} denotes the equivalent modulus
- ν denotes the Poisson ratio
- $E' = E/(1-\nu^2)$ denotes the plane stress elastic modulus
- ρ denotes the density and ρ_i the density of ice
- w_f is the weak layer fracture energy
- G is the shear modulus ($G = E/2(1+\nu)$)

7. Acknowledgements

We thank the two anonymous reviewers for their useful, constructive and detailed comments and suggestions.

References

Anderson, T. L. (2017). *Fracture mechanics: fundamentals and applications*. CRC press.

Bartelt, P. and Lehning, M. (2002). A physical snowpack model for the swiss avalanche warning: Part i: numerical model. *Cold Regions Science and Technology*, 35(3):123 – 145.

Bergfeld, B., van Herwijnen, A., Bobillier, G., Larose, E., Moreau, L., Trottet, B., Gaume, J., Cathomen, J., Dual, J., and Schweizer, J. (2021a). Crack propagation speeds in weak snowpack layers. *Journal of Glaciology*, pages 1–14.

Bergfeld, B., van Herwijnen, A., Reuter, B., Bobillier, G., Dual, J., and Schweizer, J. (2021b). Dynamic crack propagation in weak snowpack layers: insights from high-resolution, high-speed photography. *The Cryosphere*, 15(7):3539–3553.

Birkeland, K. W., van Herwijnen, A., Reuter, B., and Bergfeld, B. (2019). Temporal changes in the mechanical properties of snow related to crack propagation after loading. *Cold Regions Science and Technology*, 159:142–152.

Bobillier, G., Bergfeld, B., Dual, J., Gaume, J., van Herwijnen, A., and Schweizer, J. (2021). Micro-mechanical insights into the dynamics of crack propagation in snow fracture experiments. *Scientific Reports*, 11(1).

Boussinesq, J. (1885). *Application des potentiels a l'étude de l'équilibre et du mouvement des solides élastiques*. Gauthier-Villars.

Brown, C. and Jamieson, B. (2008). Shear strength and snowpack stability trends in non-persistant weak layers. In *Proceedings Whistler 2008 International Snow Science Workshop September 21-27, 2008*, page 939.

Brun, E., Martin, E., Simon, V., Gendre, C., and Coleou, C. (1989). An energy and mass model of snow cover suitable for operational avalanche forecasting. *Journal of Glaciology*, 35(121):333–342.

Camponovo, C. and Schweizer, J. (2001). Rheological measurements of the viscoelastic properties of snow. *Annals of Glaciology*, 32:44–50.

Capelli, A., Reiweger, I., Lehmann, P., and Schweizer, J. (2018). Fiber-bundle model with time-dependent healing mechanisms to simulate progressive failure of snow. *Phys. Rev. E*, 98:023002.

Chalmers, T. S. and Jamieson, B. (2001). Extrapolating the skier stability of buried surface hoar layers from study plot measurements. *Cold Regions Science and Technology*, 33(2):163 – 177. International Snow Science Workshop 2000.

Coléou, C. and Morin, S. (2018). Vingt-cinq ans de prévision du risque d'avalanche à météo-france. *La Météorologie*, 100:79–84.

Conway, H. and Wilbour, C. (1999). Evolution of snow slope stability during storms. *Cold Regions Science and Technology*, 30(1):67 – 77.

Denoth, A. (1980). The pendular-funicular liquid transition in snow. *Journal of Glaciology*, 25(91):93–98.

Evin, G., Sielenou, P. D., Eckert, N., Naveau, P., Hagenmuller, P., and Morin, S. (2021). Extreme avalanche cycles: Return levels and probability distributions depending on snow and meteorological conditions. *Weather and Climate Extremes*, 33:100344.

Fierz, C., R.L, A., Y, D., P, E., Greene, E., Mcclung, D., Nishimura, K., Satyawali, P., and Sokratov, S. (2009). The international classification for seasonal snow on the ground. *IHP-VII Technical Documents in Hydrology*, 83.

Föhn, P. M. (1987a). The rutschblock as a practical tool for slope stability evaluation. *IAHS Publ*, 162:223–228.

Föhn, P. M. (1987b). The stability index and various triggering mechanisms. *IAHS publication*, 162:195–214.

Gaume, J. (2012). *Prédétermination des hauteurs de départ d'avalanches. Modélisation combinée statistique-mécanique*. Theses, Université de Grenoble.

Gaume, J., Chambon, G., Eckert, N., and Naaim, M. (2013). Influence of weak-layer heterogeneity on snow slab avalanche release: application to the evaluation of avalanche release depths. *Journal of Glaciology*, 59(215):423–437.

Gaume, J., Gast, T., Teran, J., van Herwijnen, A., and Jiang, C. (2018). Dynamic anticrack propagation in snow. *Nature Communications*, 9(1):3047.

Gaume, J. and Reuter, B. (2017). Assessing snow instability in skier-triggered snow slab avalanches by combining failure initiation and crack propagation. *Cold Regions Science and Technology*, 144:6 – 15. International Snow Science Workshop 2016, Breckenridge.

Gaume, J., Schweizer, J., Herwijnen, A., Chambon, G., Reuter, B., Eckert, N., and Naaim, M. (2014). Evaluation of slope stability with respect to snowpack spatial variability. *Journal of Geophysical Research: Earth Surface*, 119(9):1783–1799.

Gaume, J., van Herwijnen, A., Chambon, G., Birkeland, K. W., and Schweizer, J. (2015). Modeling of crack propagation in weak snowpack layers using the discrete element method. *The Cryosphere*, 9(5):1915–1932.

Gaume, J., Van Herwijnen, A., CHAMBON, G., Wever, N., and Schweizer, J. (2017). Snow fracture in relation to slab avalanche release: critical state for the onset of crack propagation. *The Cryosphere*, 11(1):217–228.

Gauthier, D. and Jamieson, B. (2006). Towards a field test for fracture propagation propensity in weak snowpack layers. *Journal of Glaciology*, 52(176):164–168.

Gauthier, D. and Jamieson, B. (2008). Evaluation of a prototype field test for fracture and failure propagation propensity in weak snowpack layers. *Cold Regions Science and Technology*, 51(2):87 – 97. International Snow Science Workshop (ISSW) 2006.

Gerling, B., Löwe, H., and van Herwijnen, A. (2017). Measuring the elastic modulus of snow. *Geophysical Research Letters*, 44(21):11,088–11,096.

Giraud, G. and Navarre, J. (1995). Mepra et le risque de déclenchement accidentel d'avalanches. In *Les apports de la recherche scientifique à la sécurité neige glace et avalanche, Actes de Colloque, ANENA*.

Giraud, G., Navarre, J.-P., and Coléou, C. (2002). Estimation du risque avalancheux dans le système expert MEPRA. Unpublished work.

Griffith, A. A. (1921). VI. the phenomena of rupture and flow in solids. *Philosophical Transactions of the Royal Society of London. Series A, Containing Papers of a Mathematical or Physical Character*, 221(582-593):163–198.

Habermann, M., Schweizer, J., and Jamieson, J. B. (2008). Influence of snowpack layering on human-triggered snow slab avalanche release. *Cold Regions Science and Technology*, 54(3):176 – 182.

Hagenmuller, P. (2014). *Modélisation du comportement mécanique de la neige à partir d'images microtomographiques*. PhD thesis, Sciences de la terre et de l'univers, et de l'environnement Grenoble. Thèse de doctorat dirigée par Naaim, Mohamed.

Hagenmuller, P., Chambon, G., and Naaim, M. (2015). Microstructure-based modeling of snow mechanics: a discrete element approach. *The Cryosphere*, 9(5):1969–1982.

Hagenmuller, P., Theile, T. C., and Schneebeli, M. (2014). Numerical simulation of microstructural damage and tensile strength of snow. *Geophysical Research Letters*, 41(1):86–89.

Heierli, J., Gumbsch, P., and Zaiser, M. (2008). Anticrack nucleation as triggering mechanism for snow slab avalanches. *Science*, 321(5886):240–243.

Jamieson, B. and Johnston, C. D. (2001). Evaluation of the shear frame test for weak snowpack layers. *Annals of Glaciology*, 32:59–69.

Jamieson, B. and Schweizer, J. (2005). Using a checklist to assess manual snow profiles. *Avalanche News*, 72:57–61.

Jamieson, J. and Johnston, C. (1990). In-situ tensile tests of snow-pack layers. *Journal of Glaciology*, 36(122):102–106.

Jamieson, J. and Johnston, C. (1998). Refinements to the stability index for skier-triggered dry-slab avalanches. *Annals of Glaciology*, 26:296–302.

Jones, A., Jamieson, J., and Schweizer, J. (2006). The effect of slab and bed surface stiffness on the skier-induced shear stress in weak snowpack layers. In *Proceedings ISSW*, pages 157–164.

Jordan, R. (1991). A one-dimensional temperature model for a snow cover: Technical documentation for sntherm. 89. Technical report, Cold Regions Research and Engineering Lab Hanover NH.

Keeler, C. and Weeks, W. (1968). Investigations into the mechanical properties of alpine snow-packs. *Journal of Glaciology*, 7(50):253–271.

Kirchner, H., Michot, G., and Schweizer, J. (2002). Fracture toughness of snow in shear and tension. *Scripta Materialia*, 46(6):425–429.

Köchle, B. and Schneebeli, M. (2014). Three-dimensional microstructure and numerical calculation of elastic properties of alpine snow with a focus on weak layers. *Journal of Glaciology*, 60(222):705–713.

LaChapelle, E. R. (1977). Snow avalanches: A review of current research and applications. *Journal of Glaciology*, 19(81):313–324.

Lafaysse, M., Cluzet, B., Dumont, M., Lejeune, Y., Vionnet, V., and Morin, S. (2017). A multiphysical ensemble system of numerical snow modelling. *The Cryosphere*, 11(3):1173–1198.

Lafaysse, M., Dumont, M., Nheili, R., Viallon-Galinier, L., Carmagnola, C., Cluzet, B., Fructus, M., Hagenmuller, P., Morin, S., Spandre, P., et al. (2020). Latest scientific and technical evolutions in the crocus snowpack model. In *EGU General Assembly Conference Abstracts*, page 10217.

LeBaron, A. M. and Miller, D. A. (2016). Micromechanical analysis of energy release in snow fracture. In *Proceedings International Snow Science Workshop, Breckenridge, Colorado, 3*, pages 658–663.

Lehning, M., Bartelt, P., Brown, B., and Fierz, C. (2002a). A physical snowpack model for the swiss avalanche warning: Part iii: meteorological forcing, thin layer formation and evaluation. *Cold Regions Science and Technology*, 35(3):169 – 184.

Lehning, M., Bartelt, P., Brown, B., Fierz, C., and Satyawali, P. (2002b). A physical snowpack model for the swiss avalanche warning: Part ii.

589 snow microstructure. *Cold Regions Science and Technology*, 35(3):147 – 167.

590 Lehning, M., Fierz, C., Brown, B., and Jamieson, B. (2004). Modeling snow instability with the snow-cover model snowpack. *Annals of Glaciology*,
591 38:331–338.

592 Mayer, S., van Herwijnen, A., and Schweizer, J. (2021). A random forest model to assess snow instability from simulated snow stratigraphy. In
593 *EGU General Assembly Conference Abstracts*, pages EGU21–12259.

594 McClung, D. and Schweizer, J. (1999). Skier triggering, snow temperatures and the stability index for dry-slab avalanche initiation. *Journal of*
595 *Glaciology*, 45(150):190–200.

596 McClung, D. M. (1979). Shear fracture precipitated by strain softening as a mechanism of dry slab avalanche release. *Journal of Geophysical*
597 *Research: Solid Earth*, 84(B7):3519–3526.

598 Mede, T., Chambon, G., Hagenmuller, P., and Nicot, F. (2018). Snow failure modes under mixed loading. *Geophysical Research Letters*, 45(24).

599 Mellor, M. (1974). *A review of basic snow mechanics*. US Army Cold Regions Research and Engineering Laboratory.

600 Monti, F., Gaume, J., van Herwijnen, A., and Schweizer, J. (2016). Snow instability evaluation: calculating the skier-induced stress in a multi-
601 layered snowpack. *Natural Hazards and Earth System Sciences*, 3:4833–4869.

602 Morin, S., Horton, S., Techel, F., Bavay, M., Coléou, C., Fierz, C., Gobiet, A., Hagenmuller, P., Lafaysse, M., Ližar, M., Mitterer, C., Monti,
603 F., Müller, K., Olefs, M., Snook, J. S., van Herwijnen, A., and Vionnet, V. (2019). Application of physical snowpack models in support of
604 operational avalanche hazard forecasting: A status report on current implementations and prospects for the future. *Cold Regions Science and*
605 *Technology*, page 102910.

606 Nadreau, J.-P. and Michel, B. (1986). Yield and failure envelope for ice under multiaxial compressive stresses. *Cold Regions Science and*
607 *Technology*, 13(1):75 – 82.

608 Narita, H. (1980). Mechanical behaviour and structure of snow under uniaxial tensile stress. *Journal of Glaciology*, 26(94):275–282.

609 Nishimura, K., Baba, E., Hirashima, H., and Lehning, M. (2005). Application of the snow cover model snowpack to snow avalanche warning in
610 niseko, japan. *Cold Regions Science and Technology*, 43(1):62 – 70. Snow and Avalanches.

611 Pahaut, E. and Giraud, G. (1995). Avalanche risk forecasting in france: results and prospects. *La Météorologie*.

612 Perla, R., Beck, T., and Cheng, T. (1982). The shear strength index of alpine snow. *Cold Regions Science and Technology*, 6(1):11 – 20.

613 Podolskiy, E., Chambon, G., Naaim, M., and Gaume, J. (2013). A review of finite-element modelling in snow mechanics. *Journal of Glaciology*,
614 59(218):1189–1201.

615 Puzrin, A. M., Faug, T., and Einav, I. (2019). The mechanism of delayed release in earthquake-induced avalanches. *Proceedings of the Royal*
616 *Society A: Mathematical, Physical and Engineering Sciences*, 475(2227):20190092.

617 Reiweger, I. and Schweizer, J. (2010). Failure of a layer of buried surface hoar. *Geophysical Research Letters*, 37(24):n/a–n/a.

618 Reuter, B. and Bellaire, S. (2018). On combining snow cover and snow instability modelling. In *Proceedings of the 2018 International Snow*
619 *Science Workshop, Innsbruck, Austria*.

620 Reuter, B., Proksch, M., Löwe, H., Van Herwijnen, A., and Schweizer, J. (2019). Comparing measurements of snow mechanical properties relevant
621 for slab avalanche release. *Journal of Glaciology*, 65(249):55–67.

622 Reuter, B. and Schweizer, J. (2018). Describing snow instability by failure initiation, crack propagation, and slab tensile support. *Geophysical*
623 *Research Letters*, 45:7019–7027.

624 Reuter, B., Schweizer, J., and van Herwijnen, A. (2015). A process-based approach to estimate point snow instability. *The Cryosphere*, 9(3):837–
625 847.

626 Reuter, B., Viallon-Galinier, L., Horton, S., van Herwijnen, A., Mayer, S., Hagenmuller, P., and Morin, S. (2022). Characterizing snow instability
627 with avalanche problem types derived from snow cover simulations. *Cold Regions Science and Technology*, 194:103462.

Richter, B., Schweizer, J., Rotach, M. W., and van Herwijnen, A. (2019). Validating modeled critical crack length for crack propagation in the snow cover model snowpack. *The Cryosphere*, 13(12):3353–3366.

Roch, A. (1966a). Les déclenchements d'avalanche. *IAHS Publ.*, 69:86–99.

Roch, A. (1966b). Les variations de la résistance de la neige. *IAHS Publ.*, 69:86–99.

Rosendahl, P. L. and Weißgraeber, P. (2019a). Modeling snow slab avalanches caused by weak layer failure – part i: Slabs on compliant and collapsible weak layers. *The Cryosphere Discussions*, 2019:1–28.

Rosendahl, P. L. and Weißgraeber, P. (2019b). Modeling snow slab avalanches caused by weak layer failure – part ii: Coupled mixed-mode criterion for skier-triggered anticracks. *The Cryosphere Discussions*, 2019:1–25.

Scapozza, C. (2004). *Entwicklung eines dichte-und temperaturabhängigen Stoffgesetzes zur Beschreibung des visko-elastischen Verhaltens von Schnee*. PhD thesis, ETH Zurich.

Schweizer, J. (1999). Review of dry snow slab avalanche release. *Cold Regions Science and Technology*, 30(1-3):43–57.

Schweizer, J. (2017). On recent advances in avalanche research. *Cold Regions Science and Technology*, 144:1 – 5. International Snow Science Workshop 2016 Breckenridge.

Schweizer, J., Bellaire, S., Fierz, C., Lehning, M., and Pielmeier, C. (2006). Evaluating and improving the stability predictions of the snow cover model snowpack. *Cold Regions Science and Technology*, 46(1):52 – 59.

Schweizer, J., Bruce Jamieson, J., and Schneebeli, M. (2003). Snow avalanche formation. *Reviews of Geophysics*, 41(4).

Schweizer, J., Michot, G., and Kirchner, H. O. (2004). On the fracture toughness of snow. *Annals of Glaciology*, 38:1–8.

Schweizer, J. and Reuter, B. (2015). A new index combining weak layer and slab properties for snow instability prediction. *Natural Hazards and Earth System Sciences*, 15(1):109–118.

Schweizer, J., Reuter, B., Van Herwijnen, A., and Gaume, J. (2016a). Avalanche release 101. In *Proceedings ISSW*, pages 1–11.

Schweizer, J., Reuter, B., van Herwijnen, A., Richter, B., and Gaume, J. (2016b). Temporal evolution of crack propagation propensity in snow in relation to slab and weak layer properties. *The Cryosphere*, 10(6):2637–2653.

Schweizer, J., van Herwijnen, A., and Reuter, B. (2011). Measurements of weak layer fracture energy. *Cold Regions Science and Technology*, 69(2):139 – 144. International Snow Science Workshop 2010 Lake Tahoe.

Shapiro, L., Johnson, J., Sturm, M., and Blaisdell, G. (1997). Snow mechanics: Review of the state of knowledge and applications. Technical report, Defense technical information center.

Sielenou, P. D., Viallon-Galinier, L., Hagenmuller, P., Naveau, P., Morin, S., Dumont, M., Verfaillie, D., and Eckert, N. (2021). Combining random forests and class-balancing to discriminate between three classes of avalanche activity in the french alps. *Cold Regions Science and Technology*, page 103276.

Sigrist, C. (2006). *Measurement of fracture mechanical properties of snow and application to dry snow slab avalanche release*. PhD thesis, ETH Zurich.

Sigrist, C. and Schweizer, J. (2007). Critical energy release rates of weak snowpack layers determined in field experiments. *Geophysical Research Letters*, 34(3).

Sigrist, C., Schweizer, J., Schindler, H.-J., and Dual, J. (2006). The energy release rate of mode ii fractures in layered snow samples. *International Journal of Fracture*, 139(3):461–475.

Simenhois, R. and Birkeland, K. W. (2009). The extended column test: Test effectiveness, spatial variability, and comparison with the propagation saw test. *Cold Regions Science and Technology*, 59(2):210 – 216. International Snow Science Workshop (ISSW) 2008.

Simson, A., Löwe, H., and Kowalski, J. (2021). Elements of future snowpack modeling – part 2: A modular and extendable eulerian–lagrangian numerical scheme for coupled transport, phase changes and settling processes. *The Cryosphere Discussions*, 2021:1–33.

667 Smith, J. L. (1965). *The elastic constants, strength and density of Greenland snow as determined from measurements of sonic wave velocity*,
668 volume 167. US Army Cold Regions Research & Engineering Laboratory.
669 Srivastava, P. K., Chandel, C., Mahajan, P., and Pankaj, P. (2016). Prediction of anisotropic elastic properties of snow from its microstructure. *Cold*
670 *Regions Science and Technology*, 125:85–100.
671 Statham, G., Haegeli, P., Greene, E., Birkeland, K., Israelson, C., Tremper, B., Stethem, C., McMahon, B., White, B., and Kelly, J. (2018). A
672 conceptual model of avalanche hazard. *Natural hazards*, 90(2):663–691.
673 Stethem, C., Jamieson, B., Schaerer, P., Liverman, D., Germain, D., and Walker, S. (2003). Snow avalanche hazard in canada – a review. *Natural*
674 *Hazards*, 28(2/3):487–515.
675 Thumlert, S. and Jamieson, B. (2014). Stress measurements in the snow cover below localized dynamic loads. *Cold Regions Science and Technol-*
676 *ogy*, 106-107:28–35.
677 Trottet, B., Simenhois, R., Bobillier, G., van Herwijnen, A., Jiang, C., and Gaume, J. (2021). From sub-rayleigh to intersonic crack propagation in
678 snow slab avalanche release. In *EGU General Assembly Conference Abstracts*, pages EGU21–8253.
679 van Herwijnen, A., Gaume, J., Bair, E. H., Reuter, B., Birkeland, K. W., and Schweizer, J. (2016). Estimating the effective elastic modulus and
680 specific fracture energy of snowpack layers from field experiments. *Journal of Glaciology*, 62(236):997–1007.
681 van Herwijnen, A. and Heierli, J. (2010). A field method for measuring slab stiffness and weak layer fracture energy. In *International Snow Science*
682 *Workshop ISSW, Lake Tahoe CA, USA*, volume 17, page e22.
683 van Herwijnen, A. and Jamieson, B. (2007). Fracture character in compression tests. *Cold Regions Science and Technology*, 47(1):60 – 68. A
684 Selection of papers presented at the International Snow Science Workshop, Jackson Hole, Wyoming, September 19-24, 2004.
685 Vernay, M., Lafaysse, M., Mérindol, L., Giraud, G., and Morin, S. (2015). Ensemble forecasting of snowpack conditions and avalanche hazard.
686 *Cold Regions Science and Technology*, 120:251 – 262.
687 Vionnet, V., Brun, E., Morin, S., Boone, A., Faroux, S., Le Moigne, P., Martin, E., and Willemet, J.-M. (2012). The detailed snowpack scheme
688 crocus and its implementation in surfex v7.2. *Geoscientific Model Development*, 5(3):773–791.
689 Walters, D. J. and Adams, E. E. (2014). Quantifying anisotropy from experimental testing of radiation recrystallized snow layers. *Cold Regions*
690 *Science and Technology*, 97:72–80.
691 Wautier, A., Geindreau, C., and Flin, F. (2015). Linking snow microstructure to its macroscopic elastic stiffness tensor: A numerical homogenization
692 method and its application to 3-d images from x-ray tomography. *Geophysical Research Letters*, 42(19):8031–8041.
693 Wilhelm, C., Wiesinger, T., and Ammann, W. (2000). The avalanche winter 1999 in switzerland-an overview. Technical report, WSL/SLF Davos.
694 Zeidler, A. and Jamieson, B. (2006). Refinements of empirical models to forecast the shear strength of persistent weak snow layers part a: Layers
695 of faceted crystals. *Cold Regions Science and Technology*, 44(3):194–205.